Eur. Phys. J. C 23, 707–718 (2002)
Digital Object Identifier (DOI) 10.1007/s100520200902

THE EUROPEAN PHYSICAL JOURNAL C

Isospin breaking in low-energy charged pion–kaon elastic scattering

A. Nehme[a]

Centre de Physique Théorique, CNRS-Luminy, case 907, 13288 Marseille Cedex 09, France

Received: 19 November 2001 / Revised version: 21 December 2001 /
Published online: 5 April 2002 –

Abstract. We use chiral perturbation theory to evaluate the scattering amplitude for the process $\pi^+K^- \to \pi^+K^-$ at leading and next-to-leading orders in the chiral counting and in the presence of isospin breaking effects. We also discuss the influence of the latter on the combination of the S-wave πK scattering lengths which is relevant for the $2S$–$2P$ energy level shift of $K\pi$ atoms.

1 Introduction

The study of hadronic atoms has become a very active field. Many experiments have been conducted to provide a very precise measurement of the characteristics of these atoms [1–5]. As theory is concerned, these experimental results are highly interesting since they allow a direct access to hadronic scattering lengths by providing thus valuable information about the fundamental properties of QCD at low energy. For instance, the presently running DIRAC experiment aims at measuring the pionium lifetime τ with a 10% accuracy [1]. This would allow to determine the difference $a_0^0 - a_0^2$ with a 5% precision using the Deser-type relation [6,7]

$$\tau^{-1} \propto \left(a_0^0 - a_0^2\right)^2, \tag{1.1}$$

where a_l^I is the l-wave $\pi\pi$ scattering length in the channel with total isospin I. On the other hand, chiral perturbation theory (ChPT) [8–10] predictions for the scattering lengths have reached a precision of 2% [11]. Once the final results from DIRAC are available, ChPT will therefore be subjected to a serious test. Before confronting the experimental determination with the ChPT prediction, it is desirable to keep under control all sources of corrections to the relation (1.1). To do so, bound state calculations were performed using different approaches, such as potential scattering theory [12,13], $3D$-constraint field theory [14], the Bethe–Salpeter equation [15] and non-relativistic effective Lagrangians [16,17]. For a review on the subject and a comparison between the various methods we refer the reader to [18]. Within the framework of non-relativistic effective Lagrangians, the correct expression of relation (1.1) which includes all isospin breaking effects at leading order (LO) and next-to-leading order (NLO) was found in [19] to be

$$\tau^{-1} = \frac{1}{9}\alpha^3 \left(4M_{\pi^\pm}^2 - 4M_{\pi^0}^2 - M_{\pi^\pm}^2\alpha^2\right)^{1/2} \mathcal{A}^2(1+K). \tag{1.2}$$

In the previous equation, α stands for the fine-structure constant, $\mathcal{A}$ and K have the following expansions [19] in powers of the isospin breaking parameter $\kappa \in [\alpha, (m_d - m_u)^2]$

$$\mathcal{A} = -\frac{3}{32\pi}\mathrm{Re}A_{\mathrm{thr.}}^{+-;00} + o(\kappa), \tag{1.3}$$

$$K = \frac{1}{9}\left(\frac{M_{\pi^\pm}^2}{M_{\pi^0}^2} - 1\right)\left(a_0^0 + 2a_0^2\right)^2 - \frac{2\alpha}{3}(\ln\alpha - 1)\left(2a_0^0 + a_0^2\right) + o(\kappa). \tag{1.4}$$

The quantity of interest,

$$-\frac{3}{32\pi}\mathrm{Re}A_{\mathrm{thr.}}^{+-;00} = a_0^0 - a_0^2 + h_1(m_d - m_u)^2 + h_2\alpha, \tag{1.5}$$

represents the real part of the $\pi^+\pi^- \to \pi^0\pi^0$ scattering amplitude at order κ. It has to be calculated at threshold within ChPT to any chiral order and from which are subtracted the singular pieces behaving like q^{-1} and $\ln q$, q being the center-of-mass three-momentum. While h_1 vanishes, the coefficient h_2 was calculated in [20] at $\mathcal{O}(e^2p^2)$ where p stands for a typical external momentum and e for the electric charge.

The first DIRAC proposal [1] also planned to measure the pionium $2S$–$2P$ energy level shift ΔE. The possibility to perform such a measurement was discussed in [21]. A simultaneous measurement of τ and ΔE would allow one to pin down a_0^0 and a_0^2 separately, since [22]

$$\Delta E \propto 2a_0^0 + a_0^2. \tag{1.6}$$

Bound state calculations of the isospin breaking corrections to (1.6) were done in [13] using potential scattering theory (the main contribution comes from vacuum

[a] e-mail: nehme@cpt.univ-mrs.fr

polarization effects and can also be found in [23]). Non-relativistic effective Lagrangian calculations concerning ΔE are not available. One might however expect that they will involve the quantity $\mathrm{Re}A_{\mathrm{thr.}}^{+-;+-}$ for the corresponding $\pi^+\pi^- \to \pi^+\pi^-$ process. Electromagnetic corrections to the scattering amplitude for this process have been obtained at $\mathcal{O}(e^2p^2)$ in [24].

The proposal [1] was followed by another one extending the DIRAC project by considering the possibility of measuring the characteristics of $K\pi$ atoms with a 20% accuracy [5]. The determination of the lifetime and energy level shift for $K\pi$ atoms will give access to the S-wave πK scattering lengths $a_0^{1/2}$ and $a_0^{3/2}$, allowing one to test ChPT in the three-flavor sector. Likewise, we may expect that the relevant quantities in the final expressions for the lifetime and the level shift will involve the scattering amplitudes for $\pi^-K^+ \to \pi^0K^0$ and $\pi^+K^- \to \pi^+K^-$, respectively. In the case of the former, isospin breaking corrections have already been discussed in [25,26]. The aim of the present work is to provide a similar treatment for the latter.

This paper is organized as follows. In Sect. 2, the scattering amplitude for the process $\pi^+K^- \to \pi^+K^-$ will be calculated at NLO including isospin breaking effects and ignoring the emission of real soft photons. Being lengthy, the expression for the scattering amplitude is displayed in Appendix A. We continue with Sect. 3, where the analytic expressions for $a_0^{1/2}$ and $a_0^{3/2}$ at NLO are given. We then discuss the sensitivity of the scattering lengths to the size of the next-to-next-to-leading order (NNLO) by evaluating them using various inputs for the low-energy constants (LEC's). The threshold expansion of this process is performed in Sect. 4 where the effects of isospin breaking on the scattering lengths are evaluated. Finally, Appendix B collects the expressions for the loop functions needed in the calculation.

2 Charged pion and kaon elastic scattering

The elastic scattering process

$$\pi^+(p) + K^-(k) \to \pi^+(p') + K^-(k'), \tag{2.1}$$

is studied in terms of the Lorentz invariant Mandelstam variables

$$s = (p+k)^2, \quad t = (p-p')^2, \quad u = (p-k')^2,$$

satisfying the on-shell relation $s+t+u = 2(M_{\pi^\pm}^2 + M_{K^\pm}^2)$. These variables are related to the center-of-mass three-momentum q and scattering angle θ by

$$\begin{aligned} s &= \left(\sqrt{M_{\pi^\pm}^2+q^2} + \sqrt{M_{K^\pm}^2+q^2}\right)^2, \\ t &= -2q^2(1-\cos\theta), \\ u &= \left(\sqrt{M_{\pi^\pm}^2+q^2} - \sqrt{M_{K^\pm}^2+q^2}\right)^2 - 2q^2(1+\cos\theta). \end{aligned} \tag{2.2}$$

Let $\mathcal{M}^{+-;+-}$ and $\mathcal{M}^{++;++}$ denote the respective scattering amplitudes for the process (2.1) and its crossed channel reaction $\pi^+K^+ \to \pi^+K^+$. Then, in the isospin limit, defined by the vanishing of both the electric charge e and the up and down quark mass difference ($m_u = m_d, e = 0$), the following relations hold:

$$\begin{aligned} \mathcal{M}^{+-;+-}(s,t,u) &= \frac{2}{3}T^{1/2}(s,t,u) + \frac{1}{3}T^{3/2}(s,t,u), \\ \mathcal{M}^{++;++}(s,t,u) &= T^{3/2}(s,t,u), \end{aligned} \tag{2.3}$$

with T^I ($I = 1/2, 3/2$) being the isospin amplitudes. The above processes are related by $s \leftrightarrow u$ crossing which constrains T^I by

$$2T^{1/2}(s,t,u) = 3T^{3/2}(u,t,s) - T^{3/2}(s,t,u). \tag{2.4}$$

This is no more valid when isospin breaking effects, generated by $\delta = m_d - m_u$ and $\alpha = e^2/(4\pi)$, are switched on. In this case $s \leftrightarrow u$ crossing is expressed as

$$\mathcal{M}^{+-;+-}(s,t,u) = \mathcal{M}^{++;++}(u,t,s). \tag{2.5}$$

The effect of a non-zero value for δ can be fully analyzed by means of the strong sector chiral Lagrangian constructed in [27]. Treating isospin violation of electromagnetic origin requires the extension of ChPT in order to include virtual photons. This can be done by building operators in which photons occur as explicit dynamical degrees of freedom. The chiral Lagrangian in the electromagnetic sector, founded upon the chiral counting scheme $\mathcal{O}(e) = \mathcal{O}(p)$, was presented at NLO in [28,29].

We shall calculate the scattering amplitude (2.5) at NLO including isospin breaking effects of both strong and electromagnetic origin. Consistency requires that all of the following chiral orders should be present; $p^2, e^2, \delta, p^4, e^2p^2, \delta p^2, e^4, \delta e^2, \delta^2$. From naive dimensional estimation, we believe that the last three orders are beyond the accuracy we are looking for, and hence will be ignored in the following. Furthermore, instead of δ, our results will be expressed in terms of [27]

$$\epsilon \equiv \frac{\sqrt{3}}{4}\frac{m_d - m_u}{m_s - \hat{m}} = 1.00 \cdot 10^{-2},$$

which measures the rate of isospin violation with respect to the violation of $SU(3)$. Using Feynman graph techniques, the amplitude (2.5) can be represented at NLO by the one-particle-irreducible diagrams depicted in Fig. 1.

Although evaluating these diagrams is a simple exercise in quantum field theory, it involves different masses and thus produces lengthy expressions. These are displayed in Appendix A where we keep the contributions of the various diagrams separated. At this stage, it is useful to mention that these expressions are scale independent but infrared divergent. Since only observables are infrared safe, these infrared divergencies should cancel in the expression for the cross section where virtual photons as well as real soft photons must be taken into account. The $\mathcal{O}(\alpha)$ soft photon cross section corresponding to an arbitrary matrix element was calculated in [30]. By applying

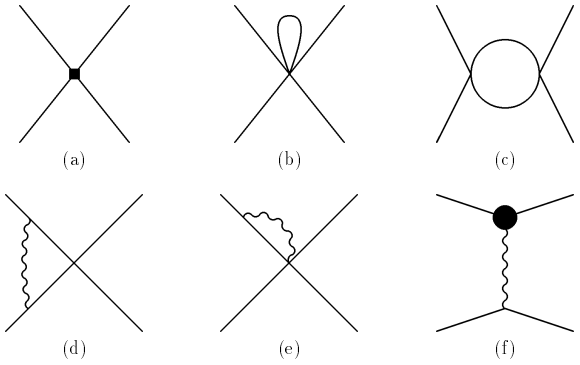

Fig. 1a–f. The various types of Feynman diagrams encountered in the charged πK scattering to one-loop order and ignoring $\mathcal{O}(e^4)$. The Born-type diagram is represented by **a**. Besides the contribution from the LEC's (the full square), it contains the tree contribution including bare mass and wave function renormalization effects. Diagram **b** represents the tadpole-type part of the amplitude. s-, t- and u-channel parts are given by diagram **c**. The one-photon contribution to the amplitude follows from diagrams **d** and **e**. We refer to diagram **f** as the form-factor-type where the full circle is made explicit in Fig. 2

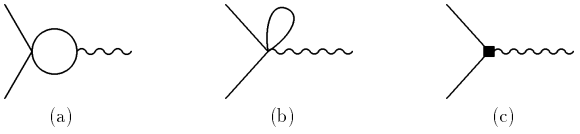

Fig. 2a–c. The electromagnetic vertex function of a charged meson to one-loop order. The full square takes into account the contribution from the LEC's just as the tree contribution including effect of wave function renormalization. Only diagrams of order $\mathcal{O}(ep^3)$ are shown

to the present calculation the general formula taken from [30], we checked that the terms in $\ln m_\gamma$ cancel with those of our expressions.

3 Scattering lengths

We are interested in the S-wave πK scattering lengths [31–33]. To this end, it is convenient to introduce the partial wave amplitudes t_l^I defined in the s-channel by

$$T^I(s,\cos\theta) = 32\pi \sum_l (2l+1) P_l(\cos\theta) t_l^I(s), \qquad (3.1)$$

where l is the angular momentum of the πK system and the P_l's are the Legendre polynomials. Near threshold the partial wave amplitudes can be parametrized in terms of scattering lengths a_l^I and slope parameters b_l^I. In normalization (3.1), the real part of the partial wave amplitudes reads

$$\mathrm{Re}\, t_l^I(s) = q^{2l}\left[a_l^I + b_l^I q^2 + \mathcal{O}(q^4)\right]. \qquad (3.2)$$

At NLO in ChPT no analytic expressions for the scattering lengths can be found anywhere. This is not the case with other approaches such as heavy-kaon ChPT [34] where the expansion parameter is M_π/M_K in addition to $M_\pi/(4\pi F_0)$ or $M_K/(4\pi F_0)$ for ChPT[1]. Obviously, at any order in both expansions, a matching between the two approaches is possible. Getting analytic expressions for $a_0^{1/2}$ and $a_0^{3/2}$ is a straightforward matter. Using the expression of isospin amplitude $T^{3/2}$ given in [35], (2.2)–(2.4) together with (3.1) and (3.2) lead to the following NLO expressions for the scattering lengths:

$$\begin{aligned}
32\pi a_0^{1/2} &= \frac{2M_{\pi^\pm}M_{K^\pm}}{F_\pi F_K}\left\{1 + \frac{4}{F_\pi F_K}(M_{\pi^\pm}^2 + M_{K^\pm}^2)L_5^r \right.\\
&- \frac{1}{1152\pi^2 F_\pi F_K}\frac{1}{M_{K^\pm}^2 - M_{\pi^\pm}^2}\\
&\times \left[9M_{\pi^\pm}^2(11M_{K^\pm}^2 - 5M_{\pi^\pm}^2)\ln\frac{M_{\pi^\pm}^2}{\mu^2}\right.\\
&+ 2M_{K^\pm}^2(9M_{K^\pm}^2 - 55M_{\pi^\pm}^2)\ln\frac{M_{K^\pm}^2}{\mu^2}\\
&\left.\left. + (36M_{K^\pm}^4 + 11M_{K^\pm}^2M_{\pi^\pm}^2 - 9M_{\pi^\pm}^4)\ln\frac{M_\eta^2}{\mu^2}\right]\right\}\\
&+ \frac{M_{\pi^\pm}^2M_{K^\pm}^2}{576\pi^2F_\pi^2F_K^2}\left\{172 + 576\pi^2\mathcal{B}(M_{K^\pm},M_{\pi^\pm})\right.\\
&- 192\pi^2\mathcal{B}(M_{K^\pm},-M_{\pi^\pm})\\
&+ 4608\pi^2\Big[4(L_1^r+L_2^r) + 2(L_3-2L_4^r) - L_5^r\\
&\left. + 2(2L_6^r + L_8^r)\Big] + \frac{1}{M_{K^\pm}^2 - M_{\pi^\pm}^2}\right.\\
&\times\left[99M_{\pi^\pm}^2\ln\frac{M_{\pi^\pm}^2}{\mu^2} - 2(67M_{K^\pm}^2 - 8M_{\pi^\pm}^2)\ln\frac{M_{K^\pm}^2}{\mu^2}\right.\\
&\left.\left. + (24M_{K^\pm}^2 - 5M_{\pi^\pm}^2)\ln\frac{M_\eta^2}{\mu^2}\right]\right\},\\
32\pi a_0^{3/2} &= -\frac{M_{\pi^\pm}M_{K^\pm}}{F_\pi F_K}\left\{1 + \frac{4}{F_\pi F_K}(M_{\pi^\pm}^2 + M_{K^\pm}^2)L_5^r\right.\\
&- \frac{1}{1152\pi^2F_\pi F_K}\frac{1}{M_{K^\pm}^2 - M_{\pi^\pm}^2}\\
&\times\left[9M_{\pi^\pm}^2(11M_{K^\pm}^2 - 5M_{\pi^\pm}^2)\ln\frac{M_{\pi^\pm}^2}{\mu^2}\right.\\
&+ 2M_{K^\pm}^2(9M_{K^\pm}^2 - 55M_{\pi^\pm}^2)\ln\frac{M_{K^\pm}^2}{\mu^2}\\
&\left.\left. + (36M_{K^\pm}^4 + 11M_{K^\pm}^2M_{\pi^\pm}^2 - 9M_{\pi^\pm}^4)\ln\frac{M_\eta^2}{\mu^2}\right]\right\}\\
&+ \frac{M_{\pi^\pm}^2M_{K^\pm}^2}{576\pi^2F_\pi^2F_K^2}\left\{172 + 384\pi^2\mathcal{B}(M_{K^\pm},-M_{\pi^\pm})\right.\\
&+ 4608\pi^2\Big[4(L_1^r+L_2^r) + 2(L_3-2L_4^r)
\end{aligned}$$

[1] Throughout this paper, M_π and M_K respectively represent the pion and kaon masses in the isospin limit, M_η the eta mass, F_0 the coupling of Goldstone bosons to axial currents in the chiral limit

Table 1. Values of the L_i^r's obtained in [40] by using large N_c arguments [41] and fitting data from [42] to ChPT predictions at NLO (set I) as also at NNLO (set II). Set III is the equivalent of set II with data coming from the preliminary analysis [43] of the E865 experiment

	set I	set II	set III
$10^3 L_1^r(M_\rho)$	0.46 ± 0.23	0.53 ± 0.25	0.43 ± 0.12
$10^3 L_2^r(M_\rho)$	1.49 ± 0.23	0.71 ± 0.27	0.73 ± 0.12
$10^3 L_3^r(M_\rho)$	-3.18 ± 0.85	-2.72 ± 1.12	-2.35 ± 0.37
$10^3 L_4^r(M_\rho)$	0 ± 0.5	0 ± 0.5	0 ± 0.5
$10^3 L_5^r(M_\rho)$	1.46 ± 0.2	0.91 ± 0.15	0.97 ± 0.11
$10^3 L_6^r(M_\rho)$	0 ± 0.3	0 ± 0.3	0 ± 0.3
$10^3 L_8^r(M_\rho)$	1.00 ± 0.20	0.62 ± 0.20	0.60 ± 0.18

$$- L_5^r + 2(2L_6^r + L_8^r)\Big] + \frac{1}{M_{K^\pm}^2 - M_{\pi^\pm}^2} \times \left[99 M_{\pi^\pm}^2 \ln\frac{M_{\pi^\pm}^2}{\mu^2} - 2(67 M_{K^\pm}^2 - 8 M_{\pi^\pm}^2)\ln\frac{M_{K^\pm}^2}{\mu^2} + (24 M_{K^\pm}^2 - 5 M_{\pi^\pm}^2)\ln\frac{M_\eta^2}{\mu^2}\right]\Bigg\}. \quad (3.3)$$

The previous expressions were obtained by using the isospin limit [36] of the Gell-Mann–Okubo relation (4.5) in the NLO contributions. F_π and F_K stand for the pion and kaon decay constants respectively. Their NLO expressions in the isospin limit can be found in [27]. For their numerical values we will use $F_\pi = 92.4\,\mathrm{MeV}$ [37] and $F_K = 1.22 F_\pi$ [38,39]. The L_i's are the LEC's weighting $\mathcal{O}(p^4)$ operators in the effective Lagrangian of [27] and values of which are collected in Table 1 with various experimental determinations. Finally, in order to obtain compact formulae, we have introduced the function $\mathcal{B}$ which expression is displayed in Appendix B. For historical reasons [31], the scattering lengths were defined in terms of the charged pion and kaon masses ($M_{\pi^\pm} = 139.570\,\mathrm{MeV}$, $M_{K^\pm} = 493.677\,\mathrm{MeV}$). Furthermore, F_0^2 was renormalized as $F_\pi F_K$ instead of F_π^2. Nevertheless, if one wishes to adopt the second choice for the renormalization of F_0, the isospin limit of (4.7) can be used.

We applied several checks to expressions (3.3). They are scale independent; the scale dependence μ of the chiral logarithms is compensated by the one governing the renormalization group equations [27] of the running couplings $L_i^r(\mu) \equiv L_i^r$. Even so, all of our expressions will be evaluated at the scale $\mu = M_\rho = 770\,\mathrm{MeV}$. Expanding expressions (3.3) to the fourth order in powers of $M_{\pi^\pm}/M_{K^\pm}$ we recover the combinations of scattering lengths obtained within the framework of heavy-kaon ChPT [34]. Using the same inputs as in [35] we come across their numerical estimates again. These expressions are consistent analytically and numerically with the combinations $2a_0^{3/2} + a_0^{1/2}$ and $a_0^{1/2} - a_0^{3/2}$ evaluated in [25].

We shall now update the numerical evaluation of [35] for the scattering lengths. All inputs have been given except the eta mass to which we assign the value $M_\eta = 547.30\,\mathrm{MeV}$. We will evaluate $a_0^{1/2}$ and $a_0^{3/2}$ using each of the sets defined in Table 1 with both renormalization choices for F_0^2. The interest of this is the following: since the difference between F_π and F_K in the NLO pieces is of $\mathcal{O}(p^6)$, then any difference in the values for the scattering lengths due to the renormalization choice for F_0 could be viewed as an indication for the size of the NNLO corrections. Note that set I and set II were obtained by fitting the same experimental data to one- and two-loop ChPT predictions respectively. It follows that the possible variation in the values for the scattering lengths due to the use of either set measures the influence of the NNLO on the NLO which, in a way, reflects the rate of convergence of the chiral expansion in powers of m_s. While Table 2 collects our numerical results for the scattering lengths, we concentrate on two specific combinations, $2a_0^{1/2} + a_0^{3/2}$ and $a_0^{1/2} - a_0^{3/2}$. For the latter, the variations are about $\sim 9\%$ due to the renormalization choice for F_0 and $\sim 1\%$ ($\sim 5\%$) due to the choice of set II instead of set I with $F_0^2 = F_\pi^2$ ($F_0^2 = F_\pi F_K$). With regard to the former, the renormalization choice for F_0 induces about $\sim 17\%$ of variation versus $\sim 10\%$ due to the choice of the set for both renormalization choices. Notice that up to a 10% accuracy, the combination $a_0^{1/2} - a_0^{3/2}$ is neither altered by the renormalization choice for F_0 nor by the choice between set I and set II. This result has already been noticed in [25] where it was concluded that the theoretical prediction for $a_0^{1/2} - a_0^{3/2}$ is so clean that if this difference was accurately measured, one might or might not confirm the validity of standard three-flavor ChPT.

4 Isospin violation at NLO

The scattering lengths are well-defined quantities in the absence of radiative corrections. When virtual photons effects have to be taken into account, things must be handled with care. To prevent any confusion, we shall perform step by step the threshold expansion of the amplitude (2.5) with the help of Appendices A and B. When expanded in powers of q, the real part of (2.5) can be put in a form similar to the one used for the $\pi\pi$ scattering case [20]:

$$\mathrm{Re}\mathcal{M}^{+-;+-}(s,t,u) = \frac{M_{\pi^\pm} M_{K^\pm}}{F_\pi F_K}\frac{e^2}{4}\frac{\mu_{\pi K}}{q} + e^2\left(\frac{u-s}{t}\right) + \mathrm{Re}\mathcal{M}_{\mathrm{thr.}}^{+-;+-} + \mathcal{O}(q), \quad (4.1)$$

$$\mathrm{Re}\mathcal{M}^{++;++}(s,t,u) = \frac{M_{\pi^\pm} M_{K^\pm}}{F_\pi F_K}\frac{e^2}{4}\frac{\mu_{\pi K}}{q} + e^2\left(\frac{s-u}{t}\right) + \mathrm{Re}\mathcal{M}_{\mathrm{thr.}}^{++;++} + \mathcal{O}(q). \quad (4.2)$$

The first two terms in the right-hand side of (4.1) should be absorbed in the static characteristics of $K\pi$ atoms [44–46] by means of a bound state treatment. The term in q^{-1} is due to the Coulomb photon exchanged between the scattered particles in diagram (d) of Fig. 1. As for the term where the dependence on the Mandelstam variables is explicit, it corresponds to diagram (f) of Fig. 1 at tree level and contains, besides the dependence on θ, a singular

Table 2. ChPT predictions for the S-wave πK scattering lengths at NLO with two possible renormalization choices for F_0. Set I, set II and set III are defined in Table 1

F_0 renormalization	a_0^I	set I	set II	set III
$F_0^2 = F_\pi^2$	$a_0^{1/2}$	0.214 ± 0.016	0.202 ± 0.018	0.203 ± 0.013
	$a_0^{3/2}$	-0.0557 ± 0.0166	-0.0660 ± 0.0185	-0.0644 ± 0.0133
$F_0^2 = F_\pi F_K$	$a_0^{1/2}$	0.192 ± 0.011	0.177 ± 0.012	0.179 ± 0.009
	$a_0^{3/2}$	-0.0613 ± 0.0113	-0.0651 ± 0.0125	-0.0644 ± 0.0090

piece behaving like q^{-2}. The q- and θ-independent terms, $\mathrm{Re}\mathcal{M}_{\mathrm{thr.}}^{+-;+-}$ and $\mathrm{Re}\mathcal{M}_{\mathrm{thr.}}^{++;++}$, constitute the main topic of this work. Their isospin limit is nothing else than the threshold value of (2.3). Then, in order to keep a coherent notation, they will be written in the following as

$$\mathrm{Re}\mathcal{M}_{\mathrm{thr.}}^{+\mp;+\mp} = 32\pi a_0(+\mp;+\mp),$$

where

$$\begin{aligned} a_0(+-;+-) &= \frac{1}{3}\left(2a_0^{1/2} + a_0^{3/2}\right) + \Delta a_0(+-;+-), \\ a_0(++;++) &= a_0^{3/2} + \Delta a_0(++;++), \end{aligned} \tag{4.3}$$

and the NLO expressions (3.3) were used for $a_0^{1/2}$ and $a_0^{3/2}$. Let us turn towards the calculation of the isospin breaking quantities Δa_0. To begin with, we express the isospin limit masses M_π and M_K figuring at NLO in terms of charged and neutral masses as

$$M_\pi^2 \to M_{\pi^0}^2, \quad 2M_K^2 \to M_{K^\pm}^2 + M_{K^0}^2 - \gamma(M_{\pi^\pm}^2 - M_{\pi^0}^2), \tag{4.4}$$

where γ takes into account any deviation from Dashen's theorem [47] for which $\gamma = 1$. Although our results correspond to $\gamma = 1$, we will use the value $\gamma = 1.84$ [48] as an indicator for their sensitivity to the violation of the Dashen theorem [49]. Furthermore, for simplification, the modified Gell-Mann–Okubo relation

$$3M_\eta^2 \to 2(M_{K^\pm}^2 + M_{K^0}^2) - (2M_{\pi^\pm}^2 - M_{\pi^0}^2), \tag{4.5}$$

will be used everywhere except in the arguments of the chiral logarithms where the eta mass is assigned to its physical value. Nevertheless, in the final results, the effect of ignoring (4.5) will also be considered. Next, still by convention, the isospin limit is defined in terms of the charged pion and kaon masses; the neutral ones should be replaced according to

$$M_{\pi^0}^2 \to M_{\pi^\pm}^2 - \Delta_\pi, \quad M_{K^0}^2 \to M_{K^\pm}^2 - \Delta_K.$$

The advantage of such a procedure is that, when expanding a_0 in powers of Δ_π and Δ_K, the zeroth order in the expansion is automatically defined in terms of charged masses and reproduces the expression for the corresponding combination of scattering lengths as given by (4.3) and (3.3). Although sufficient for our purposes, the expansion to first order in Δ_π and Δ_K is somewhat tedious, especially when considering the loop functions. The corresponding expansions of the latter are collected in Appendix B. From this, the last step is achieved by replacing Δ_π and Δ_K in the NLO terms by their LO expressions

$$\Delta_\pi \to 2Z_0 e^2 F_0^2, \quad \Delta_K \to 2Z_0 e^2 F_0^2 - \frac{4\epsilon}{\sqrt{3}}(M_K^2 - M_\pi^2),$$

which allow the following decomposition to be made:

$$\begin{aligned} 32\pi\Delta a_0(+-;+-) \equiv{}& \frac{\Delta_\pi}{F_\pi F_K} + \frac{\epsilon}{\sqrt{3}}\delta_\epsilon^{+-;+-} \\ &+ 2Z_0 e^2 F_0^2 \delta_{Z_0 e^2}^{+-;+-} + e^2 \delta_{e^2}^{+-;+-}, \\ 32\pi\Delta a_0(++;++) \equiv{}& \frac{\Delta_\pi}{F_\pi F_K} + \frac{\epsilon}{\sqrt{3}}\delta_\epsilon^{++;++} \\ &+ 2Z_0 e^2 F_0^2 \delta_{Z_0 e^2}^{++;++} + e^2 \delta_{e^2}^{++;++}. \end{aligned} \tag{4.6}$$

Once more, the renormalization choice for F_0 was fixed to $F_0^2 = F_\pi F_K$ with the possibility of renormalizing as $F_0^2 = F_\pi^2$ offered by the relation

$$\begin{aligned} \frac{1}{F_\pi F_K} = \frac{1}{F_\pi^2}\Bigg\{ & 1 + \frac{4}{F_\pi^2}(M_{\pi^\pm}^2 - M_{K^\pm}^2)L_5^r \\ & - \frac{1}{128\pi^2 F_\pi^2}\left[5M_{\pi^\pm}^2 \ln\frac{M_{\pi^\pm}^2}{\mu^2} - 2M_{K^\pm}^2 \ln\frac{M_{K^\pm}^2}{\mu^2}\right. \\ & \left. - (4M_{K^\pm}^2 - M_{\pi^\pm}^2)\ln\frac{M_\eta^2}{\mu^2}\right] \\ & - \frac{\Delta_\pi}{F_\pi^2}\left[2L_5^r - \frac{1}{128\pi^2}\left(4 + 5\ln\frac{M_\pi^2}{\mu^2} - \ln\frac{M_K^2}{\mu^2} - \ln\frac{M_\eta^2}{\mu^2}\right)\right] \\ & + \frac{\Delta_K}{F_\pi^2}\left[2L_5^r - \frac{1}{128\pi^2}\left(1 + \ln\frac{M_K^2}{\mu^2} + 2\ln\frac{M_\eta^2}{\mu^2}\right)\right]\Bigg\}. \end{aligned} \tag{4.7}$$

One should note that the consistency of the chiral power counting scheme requires that the mesons masses appearing in (4.6) be set to their isospin limit. Using instead physical masses induces corrections of higher order and thus beyond the accuracy needed for the present work.

The isospin breaking term in (4.6) generated by the difference between m_u and m_d is given by

$$\begin{aligned} \delta_\epsilon^{+\mp;+\mp} = \mp\frac{M_\pi M_K}{288\pi^2 F_\pi^2 F_K^2}\Bigg\{ & -2304\pi^2(M_K^2 - M_\pi^2)L_5^r \\ & + \frac{1}{4M_K^2 - M_\pi^2}\Big[36M_K^4 + 563M_\pi^2 M_K^2 - 135M_\pi^4 \end{aligned}$$

$$
\begin{aligned}
&- 576\pi^2 M_\pi^2 M_K^2 \mathcal{B}(M_K, \pm M_\pi)\Big] \\
&+ \frac{1}{M_K^2 - M_\pi^2}\left[27M_\pi^2(8M_K^2 + M_\pi^2)\ln\frac{M_\pi^2}{\mu^2}\right. \\
&+ (9M_K^4 - 274M_\pi^2 M_K^2 + 9M_\pi^4)\ln\frac{M_K^2}{\mu^2} \\
&+ \left.(18M_K^4 + 4M_\pi^2 M_K^2 - 9M_\pi^4)\ln\frac{M_\eta^2}{\mu^2}\right]\Bigg\} \\
&+ \frac{M_\pi^2 M_K^2}{288\pi^2 F_\pi^2 F_K^2}\Bigg\{\frac{8}{4M_K^2 - M_\pi^2}\Big[68M_K^2 - 19M_\pi^2 \\
&- 12\pi^2(32M_K^2 - 5M_\pi^2)\mathcal{B}(M_K, \pm M_\pi)\Big] \\
&+ \frac{1}{M_K^2 - M_\pi^2}\left[9(6M_K^2 + 19M_\pi^2)\ln\frac{M_\pi^2}{\mu^2}\right. \\
&- 128(M_K^2 + M_\pi^2)\ln\frac{M_K^2}{\mu^2} \\
&+ \left.(74M_K^2 - 43M_\pi^2)\ln\frac{M_\eta^2}{\mu^2}\right]\Bigg\}. \qquad (4.8)
\end{aligned}
$$

The isospin violating term due to the electromagnetic difference between charged and neutral mesons masses squared is found to read

$$
\begin{aligned}
&\delta_{Z_0 e^2}^{+\mp;+\mp} = \pm\frac{M_\pi M_K}{1152\pi^2 F_\pi^2 F_K^2} \\
&\times\Bigg\{471\delta_{+\mp} - 768\pi^2[12L_5^r - \mathcal{B}(M_K, \pm M_\pi)] \\
&- \frac{64M_K^2}{4M_K^2 - M_\pi^2}[1 - 18\pi^2\mathcal{B}(M_K, \pm M_\pi)] \\
&+ \frac{1}{M_K^2 - M_\pi^2}\Bigg[-471\Delta_{\pi K}\delta_{-\mp} - 38M_K^2 \\
&- 288\pi^2 M_K^2\mathcal{B}(M_K, \pm M_\pi) \\
&+ 27(M_K^2 + 9M_\pi^2)\ln\frac{M_\pi^2}{\mu^2} - 2(161M_K^2 + 11M_\pi^2)\ln\frac{M_K^2}{\mu^2} \\
&+ (43M_K^2 + 31M_\pi^2)\ln\frac{M_\eta^2}{\mu^2}\Bigg]\Bigg\} \\
&+ \frac{1}{1152\pi^2 F_\pi^2 F_K^2}\frac{M_\pi^2 M_K^2}{M_K^2 - M_\pi^2} \\
&\times\Bigg[78 + 9216\pi^2 L_5^r - 864\pi^2\mathcal{B}(M_K, \pm M_\pi) \\
&+ 81\ln\frac{M_\pi^2}{\mu^2} + 110\ln\frac{M_K^2}{\mu^2} - 11\ln\frac{M_\eta^2}{\mu^2}\Bigg] - \frac{1}{1152\pi^2 F_\pi^2 F_K^2} \\
&\times\frac{M_\pi^4}{M_K^2 - M_\pi^2}\left[64 + 9216\pi^2[2L_4^r + L_5^r - 2(2L_6^r + L_8^r)]\right. \\
&+ \left.63\ln\frac{M_\pi^2}{\mu^2} - 5\ln\frac{M_\eta^2}{\mu^2}\right] - \frac{M_K^4}{576\pi^2 F_\pi^2 F_K^2} \\
&\times\Bigg\{\frac{64}{4M_K^2 - M_\pi^2}[1 + 18\pi^2\mathcal{B}(M_K, \pm M_\pi)] \\
&- \frac{1}{M_K^2 - M_\pi^2}\Bigg[12 + 9216\pi^2(L_4^r - 2L_6^r - L_8^r) \qquad (4.9) \\
&+ 288\pi^2\mathcal{B}(M_K, \pm M_\pi) - 27\ln\frac{M_K^2}{\mu^2} - 34\ln\frac{M_\eta^2}{\mu^2}\Bigg]\Bigg\},
\end{aligned}
$$

with δ_{ij} representing the Kronecker symbol. Finally, virtual photons induce the following correction

$$
\begin{aligned}
&\delta_{e^2}^{+\mp;+\mp} = \pm\frac{M_\pi M_K}{144\pi^2 F_\pi F_K}\frac{1}{M_K^2 - M_\pi^2} \\
&\times\Bigg\{6[5M_K^2 + 11M_\pi^2 - 384\pi^2(M_K^2 - M_\pi^2)L_9^r] \\
&- 128\pi^2(M_K^2 - M_\pi^2) \\
&\times(3K_1^r + 3K_2^r - 18K_3^r - 9K_4^r + 4K_5^r - 5K_6^r) \\
&+ \frac{3}{M_K^2 - M_\pi^2}\Bigg[(11M_K^4 + 9M_K^2 M_\pi^2 + 12M_\pi^4)\ln\frac{M_\pi^2}{\mu^2} \\
&+ (4M_K^4 - 39M_K^2 M_\pi^2 + 3M_\pi^4)\ln\frac{M_K^2}{\mu^2}\Bigg]\Bigg\} - \frac{M_\pi^2 M_K^2}{16\pi^2 F_\pi F_K} \\
&\times\frac{1}{M_K^2 - M_\pi^2}\Bigg\{36 - 32\pi^2(2K_3^r - K_4^r - 4K_{10}^r - 4K_{11}^r) \\
&+ \frac{1}{M_K^2 - M_\pi^2}\Bigg[(9M_K^2 + 23M_\pi^2)\ln\frac{M_\pi^2}{\mu^2} \\
&- 5(3M_K^2 + 4M_\pi^2)\ln\frac{M_K^2}{\mu^2}\Bigg]\Bigg\} + \frac{2M_\pi^4}{3F_\pi F_K}\frac{1}{M_K^2 - M_\pi^2} \\
&\times(12K_2^r - 6K_3^r + 3K_4^r + K_5^r + 7K_6^r \\
&- 12K_8^r - 6K_{10}^r - 6K_{11}^r) + \frac{M_K^4}{48\pi^2 F_\pi F_K} \\
&\times\frac{1}{M_K^2 - M_\pi^2}\Bigg[12 - 32\pi^2(12K_2^r + K_5^r + 7K_6^r - 12K_8^r \\
&- 18K_{10}^r - 18K_{11}^r) - \frac{9M_K^2}{M_K^2 - M_\pi^2}\ln\frac{M_K^2}{\mu^2}\Bigg]. \qquad (4.10)
\end{aligned}
$$

It is important to emphasize that the virtual photon contribution, as can be seen from (4.10), is safe from infrared divergencies. The dependence on m_γ appears at higher orders in the expansions (4.1) and (4.2) in power of q. This fact has already been noticed in [20].

For the numerical estimate of the isospin breaking effects we use $M_{\pi^0}^2 = 134.976\,\mathrm{MeV}$, $M_{K^0}^2 = 497.672\,\mathrm{MeV}$ and the values of the L_i^r's corresponding to set II of Table 1 as our favorite ones. Concerning the LEC L_9 entering the expressions for the electromagnetic form factors of the pion and the kaon, its value will be taken as $L_9^r = (6.9 \pm 0.7)\cdot 10^{-3}$. For the LEC's in the electromagnetic sector, their central values correspond to the ones quoted in [50] where large N_c arguments [41] and resonance saturation were used. Moreover, an uncertainty of

$\pm 1/(16\pi^2)$, coming from naive dimensional analysis, will be attributed to each of the K_i^r's. In order to compare the order of magnitude for the scattering lengths and the isospin breaking corrections to those at NLO, let us recall the following combinations from Table 2 corresponding to the renormalization choice $F_0^2 = F_\pi F_K$:

$$\frac{1}{3}\left(2a_0^{1/2} + a_0^{3/2}\right) = 0.096 \pm 0.012,$$
$$a_0^{3/2} = -0.0651 \pm 0.0125. \qquad (4.11)$$

For the process $\pi^+K^- \to \pi^+K^-$, we thus obtain the following estimation for the isospin breaking effects:

$$\frac{1}{32\pi}\frac{\Delta_\pi}{F_\pi F_K} = 1.2 \times 10^{-3},$$
$$\frac{1}{32\pi}\frac{\epsilon}{\sqrt{3}}\delta_\epsilon^{+-;+-} = (2.3 \pm 0.1) \times 10^{-4},$$
$$\frac{1}{32\pi}2Z_0e^2F_0^2\delta_{Z_0e^2}^{+-;+-} = (1.4 \pm 3.9) \times 10^{-4},$$
$$\frac{1}{32\pi}e^2\delta_{e^2}^{+-;+-} = (-3.8 \pm 31) \times 10^{-4}.$$

From this we deduce that

$$a_0(+-;+-) = 0.097 \pm 0.013, \qquad (4.12)$$

indicating that the isospin breaking effects induce a correction on the combination $2a_0^{1/2} + a_0^{3/2}$ amounting to 1%. As for the process $\pi^+K^+ \to \pi^+K^+$, the results are

$$\frac{1}{32\pi}\frac{\Delta_\pi}{F_\pi F_K} = 1.2 \times 10^{-3},$$
$$\frac{1}{32\pi}\frac{\epsilon}{\sqrt{3}}\delta_\epsilon^{++;++} = (-1.4 \pm 0.1) \times 10^{-4},$$
$$\frac{1}{32\pi}2Z_0e^2F_0^2\delta_{Z_0e^2}^{++;++} = (-3.3 \pm 3.9) \times 10^{-4},$$
$$\frac{1}{32\pi}e^2\delta_{e^2}^{++;++} = (12.7 \pm 31) \times 10^{-4},$$

leading to

$$a_0(++;++) = -0.0631 \pm 0.0129. \qquad (4.13)$$

Although the size of the correction on $a_0^{3/2}$ is slightly bigger ($\sim 3\%$), it is the former combination, (4.12), that is expected to enter the expression for the $2S$–$2P$ energy level shift for $K\pi$ atoms. Before concluding let us comment on the effect induced on these results by deviations from the Gell-Mann–Okubo relation and from Dashen's theorem. If one uses the physical eta mass instead of (4.5), the central value in (4.12) increases by ~ 0.0002. On the other hand, variations of γ in (4.4) between 1 to 1.84 cause deviations of order $\sim 10^{-5}$. Accordingly, deviations from both Gell-Mann–Okubo relation and Dashen theorem induce corrections which are beyond the accuracy we are considering here.

5 Conclusions

This work was devoted to the study at NLO of isospin breaking effects on the combination $2a_0^{1/2} + a_0^{3/2}$ of S-wave πK scattering lengths which is relevant for the $2S$–$2P$ energy level shift of $K\pi$ atoms. We first gave analytic expressions for the scattering lengths which allowed to evaluate them using several sets for the values of the LEC's and with both replacements $F_0^2 \to F_\pi F_K$ and $F_0^2 \to F_\pi^2$. The particularity of these sets is that set I and set II for instance were determined by fitting the same experimental data to one- and two- loop ChPT expressions. For the value of the afore-mentioned combination we obtained a variation amounting to $\sim 17\%$ due to the choice for the replacement of F_0^2. As for the choice between the two sets, it induces a 10% variation. These numbers can be used as indicators for the size of the NNLO corrections as well as for the rate of convergence of the chiral expansion in powers of m_s. We proceeded by performing, in parallel with what has been done for the $\pi\pi$ scattering case, the threshold expansion of the scattering amplitude for the process $\pi^+K^- \to \pi^+K^-$ in the presence of photons. After subtracting singular pieces, we evaluated the isospin breaking corrections to the combination and noticed two features.

(i) Though the NLO corrections of both strong and electromagnetic origin are one order of magnitude less than the LO ones, they cancel each other in the end.
(ii) Their central value represents $\sim 1\%$ of the NLO value for the combination $2a_0^{1/2} + a_0^{3/2}$ and the uncertainty affecting them is negligible with respect to the one coming from the LEC's in the strong sector.

Acknowledgements. The author is grateful to M. Knecht for suggesting this study, for constant encouragement, precious comments and valuable advice both on the content and the presentation of the document. The author wishes to thank H. Sazdjian for enjoyable discussions, P. Talavera for helpful and appreciated comments.

Appendix

A Scattering amplitude

The amplitude (2.5) will be devided into seven parts depending on the nature of the corresponding Feynman diagrams

$$\mathcal{M}^{+-;+-} = \mathcal{M}^{\text{Born}} + \mathcal{M}^{\text{tadpole}} + \mathcal{M}^{s-\text{channel}} + \mathcal{M}^{t-\text{channel}} + \mathcal{M}^{u-\text{channel}} + \mathcal{M}^{\text{one-photon}} + \mathcal{M}^{\text{formfactor}}. \qquad (A.1)$$

We distinguish three contributions to the Born part of the amplitude (diagram (a) in Fig. 1)

$$\mathcal{M}^{\text{Born}} = \mathcal{M}^{\text{Born}}_{\text{tree}} + \mathcal{M}^{\text{Born}}_{p^4} + \mathcal{M}^{\text{Born}}_{e^2p^2}.$$

The tree contribution, denoted by $\mathcal{M}^{\text{Born}}_{\text{tree}}$, accounts for the four-meson vertex derived from the leading order (LO)

Lagrangian. Bare masses and meson wave functions being renormalized, the result is as follows:

$$
\begin{aligned}
\mathcal{M}_{\text{tree}}^{\text{Born}} &= \frac{1}{2F_0^2}(M_{\pi^\pm}^2 + M_{K^\pm}^2 - u) + \frac{\Delta_\pi}{F_0^2} \\
&+ \frac{1}{2F_0^2}(M_{\pi^\pm}^2 + M_{K^\pm}^2 - u) \\
&\times \left\{ \frac{1}{6}(5\mu_{\pi^0} + 3\mu_\eta + 4\mu_{K^0} + 6\mu_{\pi^\pm} + 6\mu_{K^\pm}) \right. \\
&- \frac{8}{F_0^2}[2(M_\pi^2 + 2M_K^2)L_4^r + (M_\pi^2 + M_K^2)L_5^r] \\
&+ 2e^2 \left[-\frac{1}{8\pi^2} - \frac{1}{16\pi^2}\left(\ln\frac{m_\gamma^2}{M_\pi^2} + \ln\frac{m_\gamma^2}{M_K^2}\right) \right. \\
&- 2F_0^2\tilde{\mu}_\pi - 2F_0^2\tilde{\mu}_K - \frac{4}{9}(6K_1^r + 6K_2^r + 5K_5^r + 5K_6^r)\Big] \\
&\left. - \frac{\epsilon}{\sqrt{3}}(\mu_\eta - \mu_\pi) + \frac{16}{F_0^2}\left(\frac{\epsilon}{\sqrt{3}}\right)(M_K^2 - M_\pi^2)L_5^r \right\} \\
&+ \frac{M_{K^\pm}^2}{6F_0^2}\left\{ -\frac{2}{3}\mu_\eta + \frac{2\epsilon}{\sqrt{3}}(\mu_\eta - \mu_\pi) \right. \\
&+ \frac{16}{F_0^2}\left(\frac{\epsilon}{\sqrt{3}}\right)(M_K^2 - M_\pi^2)(2L_8^r - L_5^r) \\
&- \frac{8}{F_0^2}[(M_\pi^2 + 2M_K^2)(2L_6^r - L_4^r) + M_K^2(2L_8^r - L_5^r)] \\
&- e^2\left[\frac{1}{4\pi^2} - 6F_0^2\tilde{\mu}_K \right. \\
&- \frac{4}{9}(6K_1^r + 6K_2^r + 5K_5^r + 5K_6^r - 6K_7 - 150K_8^r \\
&\left.\left. - 2K_9^r - 20K_{10}^r - 18K_{11}^r)\right]\right\} + \frac{M_{\pi^\pm}^2}{6F_0^2}\left\{ -\mu_{\pi^0} + \frac{1}{3}\mu_\eta \right. \\
&- \frac{8}{F_0^2}[(M_\pi^2 + 2M_K^2)(2L_6^r - L_4^r) + M_\pi^2(2L_8^r - L_5^r)] \\
&- e^2\left[\frac{7}{4\pi^2} - 42F_0^2\tilde{\mu}_\pi - \frac{4}{9}\Big(6K_1^r + 6K_2^r \right. \\
&+ 54K_3^r - 27K_4^r + 5K_5^r + 5K_6^r - 6K_7 - 78K_8^r \\
&\left.\left.\left. - 8K_9^r - 134K_{10}^r - 126K_{11}^r\Big)\right]\right\} \\
&+ \frac{\Delta_\pi}{6F_0^2}\left\{ \frac{3M_\pi^2}{8\pi^2F_0^2} + 54\mu_\pi + 28\mu_K + \frac{10}{3}\mu_\eta \right. \\
&+ \frac{16}{F_0^2}\Big[-3(M_\pi^2 + 2M_K^2)L_4^r - 3M_K^2L_5^r \\
&\left. + 2(M_\pi^2 + 2M_K^2)L_6^r + (M_\pi^2 + M_K^2)L_8^r\Big]\right\}. \qquad \text{(A.2)}
\end{aligned}
$$

As usually, the tadpole integrals read

$$
\mu_P = M_P^2\tilde{\mu}_P = \frac{M_P^2}{32\pi^2F_0^2}\ln\frac{M_P^2}{\mu^2},
$$

and the difference between the charged and neutral meson masses is symbolized by

$$
\Delta_P = M_{P^\pm}^2 - M_{P^0}^2.
$$

Note that an infrared divergent piece appears in (A.2). It comes from the charged meson wave function renormalization and is regularized by assigning a fictitious mass m_γ to the photon. The counterterms contribution $\mathcal{M}_{p^4}^{\text{Born}}$ comes from the NLO Lagrangian of the strong sector [27] and is put in the following form

$$
\begin{aligned}
\mathcal{M}_{p^4}^{\text{Born}} &= \frac{1}{F_0^4}\sum_{i=1}^{8}\mathcal{P}_iL_i^r, \\
\mathcal{P}_1 &= 8(2M_{\pi^\pm}^2 - t)(2M_{K^\pm}^2 - t), \\
\mathcal{P}_2 &= 4[(\Sigma_{\pi^-K^+} - s)^2 + (\Sigma_{\pi^-K^+} - u)^2], \\
\mathcal{P}_3 &= 2(2M_{\pi^\pm}^2 - t)(2M_{K^\pm}^2 - t) + 2(\Sigma_{\pi^-K^+} - s)^2, \\
\mathcal{P}_4 &= -\frac{2}{3}\left[M_\pi^2 + 14M_K^2 - \frac{24\epsilon}{\sqrt{3}}(M_K^2 - M_\pi^2)\right] \\
&\quad \times (2M_{\pi^\pm}^2 - t) - \frac{2}{3}(13M_\pi^2 + 2M_K^2)(2M_{K^\pm}^2 - t) \\
&\quad - \frac{4}{3}(M_\pi^2 + 2M_K^2)(\Sigma_{\pi^-K^+} - s) \\
&\quad + \frac{8}{3}(M_\pi^2 + 2M_K^2)(\Sigma_{\pi^-K^+} - u), \\
\mathcal{P}_5 &= -\frac{2}{3}(3M_{\pi^0}^2 + M_{K^\pm}^2 - \Delta_\pi)(2M_{K^\pm}^2 - t) \\
&\quad - \frac{2}{3}(M_{\pi^0}^2 + 3M_{K^\pm}^2 - 3\Delta_\pi)(2M_{\pi^\pm}^2 - t) \\
&\quad - \frac{8}{3}(M_{\pi^0}^2 + M_{K^\pm}^2 - \Delta_\pi)(\Sigma_{\pi^-K^+} - s) \\
&\quad + \frac{4}{3}(M_{\pi^0}^2 + M_{K^\pm}^2 - \Delta_\pi)(\Sigma_{\pi^-K^+} - u), \\
\mathcal{P}_6 &= \frac{8}{3}\left[2M_K^4 + 15M_\pi^2M_K^2 + M_\pi^4 \right. \\
&\quad \left. - \frac{2\epsilon}{\sqrt{3}}(2M_K^4 + 11M_\pi^2M_K^2 - 13M_\pi^4)\right], \\
\mathcal{P}_7 &= 0, \\
\mathcal{P}_8 &= \frac{8}{3}\left[M_K^4 + 6M_\pi^2M_K^2 + M_\pi^4 \right. \\
&\quad \left. - \frac{4\epsilon}{\sqrt{3}}(M_K^4 + 2M_\pi^2M_K^2 - 3M_\pi^4)\right], \qquad \text{(A.3)}
\end{aligned}
$$

where

$$
\Sigma_{PQ} = M_P^2 + M_Q^2.
$$

Finally, $\mathcal{M}_{e^2p^2}^{\text{Born}}$ represents the counterterms contribution of $\mathcal{O}(e^2p^2)$. It springs up from the NLO Lagrangian in the electromagnetic sector and reads

$$
\mathcal{M}_{e^2p^2}^{\text{Born}} = \frac{2e^2}{27F_0^2}\Big(12K_1^r + 12K_2^r + 54K_3^r + 27K_4^r
$$

$$
\begin{aligned}
&+ 10K_5^r + 10K_6^r\Big)(\Sigma_{\pi K} - u) - \frac{2e^2}{27F_0^2}\Big(6K_1^r + 6K_2^r \\
&+ 54K_3^r + 27K_4^r - 4K_5^r + 50K_6^r\Big)(\Sigma_{\pi K} - s) \\
&- \frac{4e^2}{27F_0^2}(3K_1^r + 57K_2^r + 7K_5^r + 34K_6^r)(\Sigma_{\pi K} - t) \\
&+ \frac{4e^2}{27F_0^2}\Big[3(M_\pi^2 + M_K^2)K_7 + 3(31M_\pi^2 + 43M_K^2)K_8^r \\
&+ (4M_\pi^2 + M_K^2)K_9^r + (94M_\pi^2 + 91M_K^2)K_{10}^r \\
&+ 90(M_\pi^2 + M_K^2)K_{11}^r\Big]. \qquad \text{(A.4)}
\end{aligned}
$$

The tadpole-type part of the amplitude is provided by diagram (b) in Fig. 1. Its result is shown by keeping apart individual contributions from each meson loop

$$
\begin{aligned}
\mathcal{M}^{\text{tadpole}} &= \frac{\mu_{\pi^0}}{36F_0^2}\Bigg[6u - t + 6\Delta_{\pi^-K^+} - 24\Delta_\pi \\
&+ \frac{2\epsilon}{\sqrt{3}}(3t + 2M_\pi^2 + 4M_K^2)\Bigg] \\
&+ \frac{\mu_\eta}{36F_0^2}\Bigg[6u - 3t - 6M_{\pi^\pm}^2 + 2M_{K^\pm}^2 - 20\Delta_\pi \\
&- \frac{6\epsilon}{\sqrt{3}}(t - 2M_\pi^2 + 4M_K^2)\Bigg] \\
&+ \frac{\mu_{\pi^\pm}}{18F_0^2}(12u + 3t - 8M_{\pi^\pm}^2 - 12M_{K^\pm}^2 - 72\Delta_\pi) \\
&+ \frac{\mu_{K^0}}{9F_0^2}\Bigg[-2t + 2M_{K^\pm}^2 + M_{\pi^\pm}^2 - 3\Delta_\pi \\
&+ \frac{4\epsilon}{\sqrt{3}}(M_K^2 - M_\pi^2)\Bigg] \\
&+ \frac{\mu_{K^\pm}}{18F_0^2}(12u + 3t - 12M_{\pi^\pm}^2 - 8M_{K^\pm}^2 - 72\Delta_\pi). \qquad \text{(A.5)}
\end{aligned}
$$

Concerning the unitary corrections following from diagram (b) and its two crossed ones in Fig. 1, they will be separated according to the channel specifying each crossed diagram. Moreover, the contribution of each channel will be divided into parts labelled by the kind of particles propagating inside the loop. For instance, in the s-channel

$$
\mathcal{M}^{s-\text{channel}} = \mathcal{M}_{\pi^-K^+}^{s-\text{channel}} + \mathcal{M}_{\pi^0K^0}^{s-\text{channel}} + \mathcal{M}_{\eta K^0}^{s-\text{channel}},
$$

where

$$
\begin{aligned}
\mathcal{M}_{\pi^-K^+}^{s-\text{channel}} &= \frac{1}{36F_0^4}\Bigg\{6F_0^2\mu_{K^\pm}(s - \Delta_{\pi^-K^+} + 4\Delta_\pi) \\
&+ (s + \Delta_{\pi^-K^+} + 6\Delta_\pi)^2\bar{B}(M_{\pi^\pm}^2, M_{K^\pm}^2; s) \\
&+ 2(s - 3\Delta_{\pi^-K^+})(s + \Delta_{\pi^-K^+} + 6\Delta_\pi)\bar{B}_1(M_{\pi^\pm}^2, M_{K^\pm}^2; s) \\
&+ (s - 3\Delta_{\pi^-K^+})^2\bar{B}_{21}(M_{\pi^\pm}^2, M_{K^\pm}^2; s) \\
&+ 2s[2M_{\pi^\pm}^2 - t + 4(u - t - \Delta_{\pi^-K^+})] \\
&\times \bar{B}_{22}(M_{\pi^\pm}^2, M_{K^\pm}^2; s)\Bigg\}
\end{aligned}
$$

$$
\begin{aligned}
\mathcal{M}_{\pi^0K^0}^{s-\text{channel}} &= \frac{1}{8F_0^4}\Bigg\{2F_0^2\mu_{K^0}\left(1 + \frac{2\epsilon}{\sqrt{3}}\right) \\
&\times (3s - 3M_{\pi^0}^2 - M_{K^0}^2) \\
&+ \left[s - \Sigma_{\pi^0K^0} + \frac{\epsilon}{\sqrt{3}}(s - 9M_\pi^2 + 7M_K^2)\right]^2\bar{B}(M_{\pi^0}^2, M_{K^0}^2; s) \\
&+ 2\left[s - \Sigma_{\pi^0K^0} + \frac{\epsilon}{\sqrt{3}}(s - 9M_\pi^2 + 7M_K^2)\right] \\
&\times \left[s - \Delta_{\pi^-K^+} + \frac{\epsilon}{\sqrt{3}}(s + 3\Delta_{\pi K})\right]\bar{B}_1(M_{\pi^0}^2, M_{K^0}^2; s) \\
&+ \left[s - \Delta_{\pi^-K^+} + \frac{\epsilon}{\sqrt{3}}(s + 3\Delta_{\pi K})\right]^2\bar{B}_{21}(M_{\pi^0}^2, M_{K^0}^2; s) \\
&+ 2s\left[2M_{K^\pm}^2 - t + \frac{2\epsilon}{\sqrt{3}}(t - 2u + 2M_\pi^2)\right] \\
&\times \bar{B}_{22}(M_{\pi^0}^2, M_{K^0}^2; s)\Bigg\},
\end{aligned}
$$

$$
\begin{aligned}
\mathcal{M}_{\eta K^0}^{s-\text{channel}} &= \frac{1}{24F_0^4}\Bigg\{2F_0^2\mu_{K^0}\left(1 - \frac{3\epsilon}{\sqrt{3}}\right) \\
&\times \left[3s - 3M_\eta^2 - M_{K^0}^2 - \frac{3\epsilon}{\sqrt{3}}(3s - M_K^2 - 3M_\eta^2)\right] \\
&+ \left[s + 7M_\eta^2 - 9M_{K^0}^2 - \frac{\epsilon}{\sqrt{3}}(3s + 17M_\pi^2 - 23M_K^2)\right]^2 \\
&\times \bar{B}(M_\eta^2, M_{K^0}^2; s) + 2\left[s + 3\Delta_{\pi^-K^+} - \frac{3\epsilon}{\sqrt{3}}(s - \Delta_{\pi K})\right] \\
&\times \left[s + 7M_\eta^2 - 9M_{K^0}^2 - \frac{\epsilon}{\sqrt{3}}(3s + 17M_\pi^2 - 23M_K^2)\right] \\
&\times \bar{B}_1(M_\eta^2, M_{K^0}^2; s) + \left[s + 3\Delta_{\pi^-K^+} - \frac{3\epsilon}{\sqrt{3}}(s - \Delta_{\pi K})\right]^2 \\
&\times \bar{B}_{21}(M_\eta^2, M_{K^0}^2; s) + 2s\left[4u - 5t + 4M_{\pi^\pm}^2 - 2M_{K^\pm}^2\right. \\
&- \left.\frac{6\epsilon}{\sqrt{3}}(t - 2u + 2M_\pi^2)\right]\bar{B}_{22}(M_\eta^2, M_{K^0}^2; s)\Bigg\}. \qquad \text{(A.6)}
\end{aligned}
$$

The loop functions shown in (A.6) and in what follows are discussed in Appendix B; the quantity Δ_{PQ} stands for

$$
\Delta_{PQ} = M_P^2 - M_Q^2.
$$

A similar notation holds for the t- and u-channels:

$$
\begin{aligned}
\mathcal{M}^{t-\text{channel}} &= \mathcal{M}_{\pi^0\pi^0}^{t-\text{channel}} + \mathcal{M}_{\eta\eta}^{t-\text{channel}} + \mathcal{M}_{\pi^0\eta}^{t-\text{channel}} \\
&\quad + \mathcal{M}_{\pi^+\pi^-}^{t-\text{channel}} + \mathcal{M}_{K^0\bar{K}^0}^{t-\text{channel}} + \mathcal{M}_{K^+K^-}^{t-\text{channel}}, \\
\mathcal{M}^{u-\text{channel}} &= \mathcal{M}_{\pi^-K^+}^{u-\text{channel}}, \qquad \text{(A.7)}
\end{aligned}
$$

which individual parts are given by

$$
\begin{aligned}
\mathcal{M}_{\pi^0\pi^0}^{t-\text{channel}} &= \frac{1}{36F_0^4}\Bigg\{-2F_0^2\mu_{\pi^0} \\
&\times \left[-5t + 3M_{\pi^0}^2 + \frac{6\epsilon}{\sqrt{3}}(-5t + 3M_\pi^2 + 4M_K^2)\right]
\end{aligned}
$$

$$
\begin{aligned}
&+\frac{3}{2}(t-M_{\pi^0}^2)\left[3t+\frac{6\epsilon}{\sqrt{3}}(3t-4M_K^2)\right]\\
&\times\bar{B}(M_{\pi^0}^2,M_{\pi^0}^2;t)\Bigg\},\\
\mathcal{M}_{\eta\eta}^{t-\text{channel}}&=\frac{M_{\pi^0}^2}{72F_0^4}\Bigg\{12F_0^2\left(1-\frac{2\epsilon}{\sqrt{3}}\right)\mu_\eta\\
&+\left[9t-6M_\eta^2-2M_{\pi^0}^2-\frac{2\epsilon}{\sqrt{3}}(9t+8M_\pi^2-20M_K^2)\right]\\
&\times\bar{B}(M_\eta^2,M_\eta^2;t)\Bigg\},\\
\mathcal{M}_{\pi^0\eta}^{t-\text{channel}}&=-\frac{1}{12F_0^4}\left(\frac{\epsilon}{\sqrt{3}}\right)\\
&\times\Bigg\{2F_0^2\mu_\pi(5t-6M_\pi^2-2M_\eta^2)+2F_0^2\mu_\eta(5t-4\Sigma_{\pi\eta})\\
&+(3t-4M_\pi^2)(3t-3M_\eta^2-M_\pi^2)\bar{B}(M_\pi^2,M_\eta^2;t)\Bigg\},\\
\mathcal{M}_{\pi^+\pi^-}^{t-\text{channel}}&=\frac{1}{18F_0^4}\Bigg\{-\frac{3}{16\pi^2}\left(M_{\pi^\pm}^2-\frac{t}{6}\right)(s-u)\\
&+F_0^2\mu_{\pi^\pm}\left[5t+24\Delta_\pi+3(s-u)\right]\\
&+\left[\frac{9}{4}t(t+8\Delta_\pi)-3(s-u)\left(M_{\pi^\pm}^2-\frac{t}{4}\right)\right]\\
&\times\bar{B}(M_{\pi^\pm}^2,M_{\pi^\pm}^2;t)\Bigg\},\\
\mathcal{M}_{K^0\bar{K}^0}^{t-\text{channel}}&=\frac{1}{36F_0^4}\Bigg\{F_0^2\mu_{K^0}\left[5t-3(s-u)\right]\\
&+\frac{3}{16\pi^2}\left(M_{K^0}^2-\frac{t}{6}\right)(s-u)\\
&+\left[\frac{9}{4}t^2+3(s-u)\left(M_{K^0}^2-\frac{t}{4}\right)\right]\\
&\times\bar{B}(M_{K^0}^2,M_{K^0}^2;t)\Bigg\},\\
\mathcal{M}_{K^+K^-}^{t-\text{channel}}&=\frac{1}{18F_0^4}\Bigg\{F_0^2\mu_{K^\pm}\left[5t+3(s-u)+24\Delta_\pi\right]\\
&-\frac{3}{16\pi^2}\left(M_{K^\pm}^2-\frac{t}{6}\right)(s-u)\\
&+\left[\frac{9}{4}t(t+8\Delta_\pi)-3(s-u)\left(M_{K^\pm}^2-\frac{t}{4}\right)\right]\\
&\times\bar{B}(M_{K^\pm}^2,M_{K^\pm}^2;t)\Bigg\},\\
\mathcal{M}_{\pi^-K^+}^{u-\text{channel}}&=\frac{1}{9F_0^4}\Bigg\{-6F_0^2\mu_{K^\pm}(\Sigma_{\pi^-K^+}-u+2\Delta_\pi)\\
&+(2M_{\pi^\pm}^2+M_{K^\pm}^2-u+3\Delta_\pi)^2\bar{B}(M_{\pi^\pm}^2,M_{K^\pm}^2;u)\\
&-2u(2M_{\pi^\pm}^2+M_{K^\pm}^2-u+3\Delta_\pi)\bar{B}_1(M_{\pi^\pm}^2,M_{K^\pm}^2;u)\\
&+u^2\bar{B}_{21}(M_{\pi^\pm}^2,M_{K^\pm}^2;u)+u^2\bar{B}_{22}(M_{\pi^\pm}^2,M_{K^\pm}^2;u)\Bigg\}.
\end{aligned}
\tag{A.8}
$$

With regard to the one-photon contributions, they will be classified with respect to the topology of the exchanged photon

$$
\begin{aligned}
\mathcal{M}^{\text{one-photon}}=&\,\mathcal{M}_{\text{vertex-leg}}^{\text{one-photon}}+\mathcal{M}_{s-\text{channel}}^{\text{one-photon}}\\
&+\mathcal{M}_{t-\text{channel}}^{\text{one-photon}}+\mathcal{M}_{u-\text{channel}}^{\text{one-photon}}.
\end{aligned}
$$

We distinguish a tadpole-type contribution schematized by diagram (e) in Fig. 1 and for which we found

$$
\begin{aligned}
\mathcal{M}_{\text{vertex-leg}}^{\text{one-photon}}=&\frac{2e^2}{3F_0^2}\left[(u+\Delta_{\pi K})\left(-6F_0^2\tilde{\mu}_\pi+\frac{1}{4\pi^2}\right)\right.\\
&\left.+(u-\Delta_{\pi K})\left(-6F_0^2\tilde{\mu}_K+\frac{1}{4\pi^2}\right)\right].
\end{aligned}
$$

We also distinguish a unitary contribution given by diagram (d) in Fig. 1. The expressions relative to the different channels defined by the exchanged photon topology read

$$
\begin{aligned}
\mathcal{M}_{s-\text{channel}}^{\text{one-photon}}&=\frac{e^2}{3F_0^2}\Bigg\{\frac{1}{2}F_0^2\tilde{\mu}_\pi\\
&\times\left[3(t-u)-12(\Sigma_{\pi K}-u)+s-2\Delta_{\pi K}\right]+\frac{1}{2}F_0^2\tilde{\mu}_K\\
&\times\left[3(t-u)-12(\Sigma_{\pi K}-u)+s+2M_\pi^2-6M_K^2\right]\\
&+(s-3M_\pi^2-M_K^2)\bar{B}(M_\pi^2,M_K^2,s)\\
&+(3\Delta_{\pi K}-s)\bar{B}_1(M_\pi^2,M_K^2,s)\\
&+2(\Sigma_{\pi K}-s)[3(u-t)+2\Sigma_{\pi K}-s]G_{\pi K}^-(s)\\
&+8\Delta_{\pi K}(\Sigma_{\pi K}-s)G_{\pi K}^+(s)\\
&+6(\Sigma_{\pi K}-u)(\Sigma_{\pi K}-s)G_{\pi K}(s)\\
&+6(\Sigma_{\pi K}-u)\left(\frac{1}{16\pi^2}\right)\Bigg\},\\
\mathcal{M}_{t-\text{channel}}^{\text{one-photon}}&=\frac{e^2}{6F_0^2}\Bigg\{-2F_0^2\tilde{\mu}_\pi\\
&\times\left[6(\Sigma_{\pi K}-u)-\frac{3}{2}(2M_\pi^2-t)\right]\\
&-3(\Sigma_{\pi K}-u)\bar{B}(M_\pi^2,M_\pi^2,t)\\
&-\frac{1}{16\pi^2}\left[-9(\Sigma_{\pi K}-u)-\frac{1}{2}(t-8M_\pi^2)\right]\\
&+6(2M_\pi^2-t)(\Sigma_{\pi K}-u)G_{\pi\pi}(t)\\
&-\frac{3}{2}(s-u)(4M_\pi^2-3t)G_{\pi\pi}^-(t)\Bigg\}\\
&+\frac{e^2}{6F_0^2}\Bigg\{-2F_0^2\tilde{\mu}_K\left[6(\Sigma_{\pi K}-u)-\frac{3}{2}(2M_K^2-t)\right]\\
&-3(\Sigma_{\pi K}-u)\bar{B}(M_K^2,M_K^2,t)\\
&-\frac{1}{16\pi^2}\left[-9(\Sigma_{\pi K}-u)-\frac{1}{2}(t-8M_K^2)\right]
\end{aligned}
$$

$$
\begin{aligned}
&+ 6(2M_K^2 - t)(\Sigma_{\pi K} - u)G_{KK}(t) \\
&- \frac{3}{2}(s-u)(4M_K^2 - 3t)G^-_{KK}(t)\Bigg\}, \\
\mathcal{M}^{\text{one-photon}}_{u-\text{channel}} &= -\frac{e^2}{3F_0^2}\Bigg\{F_0^2\tilde{\mu}_\pi(5u - 5M_K^2 - 7M_\pi^2) \\
&+ F_0^2\tilde{\mu}_K(5u - 5M_\pi^2 - 3M_K^2) \\
&+ 2(M_K^2 - u)\bar{B}(M_\pi^2, M_K^2, u) + 2u\bar{B}_1(M_\pi^2, M_K^2, u) \\
&- 4(\Sigma_{\pi K} - u)(2\Sigma_{\pi K} - u)G^-_{\pi K}(u) \\
&- 4\Delta_{\pi K}(\Sigma_{\pi K} - u)G^+_{\pi K}(u) \qquad \text{(A.9)} \\
&+ 6(\Sigma_{\pi K} - u)^2 G_{\pi K}(u) + 6(\Sigma_{\pi K} - u)\left(\frac{1}{16\pi^2}\right)\Bigg\}.
\end{aligned}
$$

Finally, the result for diagram (f) in Fig. 1 can be put in the following form:

$$
\mathcal{M}^{\text{formfactor}} = e^2\left(\frac{u-s}{t}\right)[1 + \Gamma_\pi(t) + \Gamma_K(t)],
$$

where Γ_π and Γ_K represent the electromagnetic vertex functions for the pion and kaon respectively [51]

$$
\begin{aligned}
\Gamma_\pi(t) &= \frac{t}{F_0^2}\left[2L_9^r - \frac{1}{96\pi^2}\left(\ln\frac{M_\pi^2}{\mu^2} + \frac{1}{2}\ln\frac{M_K^2}{\mu^2}\right)\right] \\
&- \frac{2}{3F_0^2}\left[\left(M_\pi^2 - \frac{t}{4}\right)\bar{B}(M_\pi^2, M_\pi^2, t) + \frac{1}{16\pi^2}\frac{t}{12}\right] \\
&- \frac{1}{3F_0^2}\left[\left(M_K^2 - \frac{t}{4}\right)\bar{B}(M_K^2, M_K^2, t) + \frac{1}{16\pi^2}\frac{t}{12}\right], \\
\Gamma_K(t) &= \frac{t}{F_0^2}\left[2L_9^r - \frac{1}{96\pi^2}\left(\ln\frac{M_K^2}{\mu^2} + \frac{1}{2}\ln\frac{M_\pi^2}{\mu^2}\right)\right] \\
&- \frac{1}{3F_0^2}\left[\left(M_\pi^2 - \frac{t}{4}\right)\bar{B}(M_\pi^2, M_\pi^2, t) + \frac{1}{16\pi^2}\frac{t}{12}\right] \\
&- \frac{2}{3F_0^2}\left[\left(M_K^2 - \frac{t}{4}\right)\bar{B}(M_K^2, M_K^2, t) + \frac{1}{16\pi^2}\frac{t}{12}\right].
\end{aligned} \qquad \text{(A.10)}
$$

B Loop functions

The loop functions we use in our calculations follow the notations of [52]. Analytic expressions were given in [25]. For completeness we recall the expression for the following function

$$
\begin{aligned}
\mathcal{B}(x,y) &= -\frac{\sqrt{(x-y)(2x+y)}}{12\pi^2(x+y)} \\
&\times\left\{\arctan\left[\frac{\sqrt{(x-y)(2x+y)}}{2(x-y)}\right]\right. \\
&\left.+\ \arctan\left[\frac{x+2y}{2\sqrt{(x-y)(2x+y)}}\right]\right\}. \qquad \text{(B.1)}
\end{aligned}
$$

For the threshold expansion of the processes analyzed in this paper, we need the following expressions for the two-point functions defined in [25]

$$
\begin{aligned}
&\text{Re}\bar{J}(M_{\pi^\pm}^2, M_{K^\pm}^2, M_\pm^2) \\
&= \frac{1}{16\pi^2}\left(1 \mp \frac{M_{\pi^\pm}M_{K^\pm}}{M_{K^\pm}^2 - M_{\pi^\pm}^2}\ln\frac{M_{\pi^\pm}^2}{M_{K^\pm}^2}\right), \\
&\text{Re}\bar{J}(M_{\pi^0}^2, M_{K^0}^2, M_\pm^2) \\
&= \frac{1}{16\pi^2}\left(1 \mp \frac{M_{\pi^\pm}M_{K^\pm}}{M_{K^\pm}^2 - M_{\pi^\pm}^2}\ln\frac{M_{\pi^\pm}^2}{M_{K^\pm}^2}\right) \\
&+ \frac{\Delta_\pi}{32\pi^2}\left\{\frac{2}{M_K^2 - M_\pi^2}\left(2 \mp \frac{M_K}{M_\pi}\right) + \frac{1}{(M_K^2 - M_\pi^2)^2}\right. \\
&\left.\times\ [2(2M_K^2 + M_\pi^2) - (M_K \pm M_\pi)^2]\ln\frac{M_\pi^2}{M_K^2}\right\} \\
&- \frac{\Delta_K}{32\pi^2}\left\{\frac{2}{M_K^2 - M_\pi^2}\left(2 \mp \frac{M_\pi}{M_K}\right) + \frac{1}{(M_K^2 - M_\pi^2)^2}\right. \\
&\left.\times\ [2(M_K^2 + 2M_\pi^2) - (M_K \pm M_\pi)^2]\ln\frac{M_\pi^2}{M_K^2}\right\}, \\
&\text{Re}\bar{J}(M_\eta^2, M_{K^0}^2, M_\pm^2) \\
&= \frac{1}{16\pi^2}[1 + 16\pi^2\mathcal{B}(M_{K^\pm}, \pm M_{\pi^\pm})] + \frac{1}{48\pi^2}\frac{1}{M_{K^\pm}^2 - M_{\pi^\pm}^2} \\
&\times\ (5M_{K^\pm} \mp 2M_{\pi^\pm})(2M_{K^\pm} \pm M_{\pi^\pm})\ln\frac{M_\eta^2}{M_{K^\pm}^2} \\
&- \frac{1}{96\pi^2}\frac{\Delta_\pi}{M_K^2 - M_\pi^2}\left[12\pi^2\left(\frac{M_K \pm 2M_\pi}{2M_K \pm M_\pi}\right)\mathcal{B}(M_K, \pm M_\pi)\right. \\
&+ 2\left(\frac{M_K \mp M_\pi}{2M_K \mp M_\pi}\right) \\
&\left.- \left(\frac{19M_K^2 \mp 2M_K M_\pi + M_\pi^2}{M_K^2 - M_\pi^2}\right)\ln\frac{M_\eta^2}{M_K^2}\right] \\
&- \frac{1}{96\pi^2}\frac{\Delta_K}{M_K^2 - M_\pi^2}\left[12\pi^2\left(\frac{8M_K \pm 7M_\pi}{2M_K \pm M_\pi}\right)\mathcal{B}(M_K, \pm M_\pi)\right. \\
&- 2\left(\frac{16M_K \mp 7M_\pi}{2M_K \mp M_\pi}\right) \\
&\left.+ \left(\frac{37M_K^2 \mp 2M_K M_\pi - 17M_\pi^2}{M_K^2 - M_\pi^2}\right)\ln\frac{M_\eta^2}{M_K^2}\right], \qquad \text{(B.2)}
\end{aligned}
$$

and evaluated at

$$
M_\pm = M_{\pi^\pm} \pm M_{K^\pm}.
$$

Finally, we quote the expression of the infrared divergent three-point function with the corresponding cut structure needed for the calculation of diagram (d) in Fig. 1 with the various channels defined in (A.9)

$$
\begin{aligned}
&32\pi^2\lambda_{PQ}^{1/2}(p^2)G_{PQ}(p^2) = 2\text{Li}_2\left[\frac{p^2 + \Delta_{PQ} + \lambda_{PQ}^{1/2}(p^2)}{p^2 + \Delta_{PQ} - \lambda_{PQ}^{1/2}(p^2)}\right] \\
&-2\text{Li}_2\left[\frac{p^2 - \Delta_{PQ} - \lambda_{PQ}^{1/2}(p^2)}{p^2 - \Delta_{PQ} + \lambda_{PQ}^{1/2}(p^2)}\right] - \left\{\ln\left[\frac{\lambda_{PQ}(p^2)}{p^2 m_\gamma^2}\right]\right. \\
&\left.- \frac{1}{2}\ln\left[\frac{[\Delta_{PQ} - \lambda_{PQ}^{1/2}(p^2)]^2 - p^4}{[\Delta_{PQ} + \lambda_{PQ}^{1/2}(p^2)]^2 - p^4}\right] - \text{i}\pi\Theta(p^2)\right\}
\end{aligned}
$$

$$\times\Bigg\{\ln\left[\frac{[p^2-\lambda_{PQ}^{1/2}(p^2)]^2-\Delta_{PQ}^2}{[p^2+\lambda_{PQ}^{1/2}(p^2)]^2-\Delta_{PQ}^2}\right] +2\mathrm{i}\pi\Theta\left[p^2-(M_P+M_Q)^2\right]\Bigg\}. \tag{B.3}$$

In this expression, Θ stands for the Heaviside function, λ_{PQ} for the Källén function

$$\lambda_{PQ}(p^2)\equiv\left[p^2-(M_P+M_Q)^2\right]\left[p^2-(M_P-M_Q)^2\right],$$

and the dilogarithm function is defined by

$$\mathrm{Li}_2(z)\equiv-\int_0^z \mathrm{d}t\frac{\ln(1-t)}{t}.$$

Notice that in the equal mass limit ($M_P=M_Q$), the function (B.3) reduces to the one given in [20].

References

1. B. Adeva et al., CERN-SPSLC-95-1
2. D. Sigg, A. Badertscher, P.F. Goudsmit, H.J. Leisi, G.C. Oades, Nucl. Phys. A **609**, 310 (1996); H.J. Leisi, PiN Newslett. **15**, 258 (1999); H.C. Schroder et al., Phys. Lett. B **469**, 25 (1999); D. Gotta, PiN Newslett. **15**, 276 (1999)
3. W.H. Breunlich et al. [DEAR Collaboration], PiN Newslett. **15**, 266 (1999); M. Augsburger et al., Nucl. Phys. A **663**, 561 (2000)
4. M. Iwasaki et al., Phys. Rev. Lett. **78**, 3067 (1997); M. Iwasaki et al., Nucl. Phys. A **639**, 501 (1998)
5. B. Adeva et al., CERN-SPSC-2000-032
6. S. Deser, M.L. Goldberger, K. Baumann, W. Thirring, Phys. Rev. **96**, 774 (1954)
7. S.M. Bilenkii, V.H. Nguyen, L.L. Nemenov, F.G. Tkebuchava, Yad. Fiz. **10**, 812 (1969)
8. H. Leutwyler, Annals Phys. **235**, 165 (1994)
9. G. Ecker, Prog. Part. Nucl. Phys. **35**, 1 (1995)
10. A. Pich, Effective field theory, in Les Houches Summer School in Theoretical Physics, Session 68: Probing the Standard Model of Particle Interactions, edited by R. Gupta, A. Morel, E. de Rafael, F. David, Elsevier, Amsterdam (1999); hep-ph/9806303
11. G. Colangelo, J. Gasser, H. Leutwyler, Phys. Lett. B **488**, 261 (2000)
12. U. Moor, G. Rasche, W.S. Woolcock, Nucl. Phys. A **587**, 747 (1995)
13. A. Gashi, G. Rasche, G.C. Oades, W.S. Woolcock, Nucl. Phys. A **628**, 101 (1998)
14. H. Jallouli, H. Sazdjian, Phys. Rev. D **58**, 014011 (1998) [Erratum-ibid. D **58**, 099901 (1998)]; H. Sazdjian, Phys. Lett. B **490**, 203 (2000)
15. V.E. Lyubovitskij, A. Rusetsky, Phys. Lett. B **389**, 181 (1996); V.E. Lyubovitskij, E.Z. Lipartia, A.G. Rusetsky, Pisma Zh. Eksp. Teor. Fiz. **66**, 747 (1997) [JETP Lett. **66**, 783 (1997)]; M.A. Ivanov, V.E. Lyubovitskij, E.Z. Lipartia, A.G. Rusetsky, Phys. Rev. D **58**, 094024 (1998)
16. X. Kong, F. Ravndal, Phys. Rev. D **59**, 014031 (1999); X.W. Kong, F. Ravndal, Phys. Rev. D **61**, 077506 (2000); B.R. Holstein, Phys. Rev. D **60**, 114030 (1999); D. Eiras, J. Soto, Nucl. Phys. Proc. Suppl. **86**, 267 (2000) [PiN Newslett. **15**, 181 (2000)]; D. Eiras, J. Soto, Phys. Rev. D **61**, 114027 (2000)
17. J. Gasser, V.E. Lyubovitskij, A. Rusetsky, A. Gall, Phys. Rev. D **64**, 016008 (2001)
18. J. Gasser, V.E. Lyubovitskij, A. Rusetsky, Phys. Lett. B **471**, 244 (1999)
19. A. Gall, J. Gasser, V.E. Lyubovitskij, A. Rusetsky, Phys. Lett. B **462**, 335 (1999)
20. M. Knecht, R. Urech, Nucl. Phys. B **519**, 329 (1998)
21. L.L. Nemenov, V.D. Ovsyannikov, Phys. Lett. B **514**, 247 (2001)
22. G.V. Efimov, M.A. Ivanov, V.E. Lyubovitskij, Sov. J. Nucl. Phys. **44**, 296 (1986) [Yad. Fiz. **44**, 460 (1986)]
23. D. Eiras, J. Soto, Phys. Lett. B **491**, 101 (2000)
24. M. Knecht, A. Nehme, Phys. Lett. B in press, hep-ph/0201033
25. A. Nehme, P. Talavera, Phys. Rev. D **65**, 054023 (2002)
26. B. Kubis, U.G. Meissner, Nucl. Phys. A **699**, 709 (2002)
27. J. Gasser, H. Leutwyler, Nucl. Phys. B **250**, 465 (1985)
28. R. Urech, Nucl. Phys. B **433**, 234 (1995)
29. H. Neufeld, H. Rupertsberger, Z. Phys. C **68**, 91 (1995); H. Neufeld, H. Rupertsberger, Z. Phys. C **71**, 131 (1996)
30. A. Denner, Fortsch. Phys. **41**, 307 (1993)
31. S. Weinberg, Phys. Rev. Lett. **17**, 616 (1966)
32. J.A. Cronin, Phys. Rev. **161**, 1483 (1967); R.W. Griffith, Phys. Rev. **176**, 1705 (1968)
33. M. Knecht, H. Sazdjian, J. Stern, N.H. Fuchs, Phys. Lett. B **313**, 229 (1993)
34. A. Roessl, Nucl. Phys. B **555**, 507 (1999)
35. V. Bernard, N. Kaiser, U.G. Meissner, Phys. Rev. D **43**, 2757 (1991); V. Bernard, N. Kaiser, U.G. Meissner, Nucl. Phys. B **357**, 129 (1991)
36. M. Gell-Mann, Phys. Rev. **125**, 1067 (1962); S. Okubo, Prog. Theor. Phys. **27**, 949 (1962)
37. B.R. Holstein, Phys. Lett. B **244**, 83 (1990)
38. H. Leutwyler, M. Roos, Z. Phys. C **25**, 91 (1984)
39. N.H. Fuchs, M. Knecht, J. Stern, Phys. Rev. D **62**, 033003 (2000)
40. G. Amoros, J. Bijnens, P. Talavera, Nucl. Phys. B **602**, 87 (2001)
41. G. 't Hooft, Nucl. Phys. B **72**, 461 (1974); E. Witten, Nucl. Phys. B **160**, 57 (1979)
42. L. Rosselet et al., Phys. Rev. D **15**, 574 (1977)
43. P. Truol, hep-ex/0012012
44. L.L. Nemenov, Sov. J. Nucl. Phys. **41**, 629 (1985) [Yad. Fiz. 41 (1985) 980]
45. G.V. Efimov, M.A. Ivanov, V.E. Lyubovitskij, JETP Lett. **45**, 672 (1987) [Pisma Zh. Eksp. Teor. Fiz. **45**, 526 (1987)]
46. A.A. Belkov, V.N. Pervushin, F.G. Tkebuchava, Yad. Fiz. **44**, 466 (1986) [Sov. J. Nucl. Phys. **44**, 300 (1986)]
47. R.F. Dashen, Phys. Rev. **183**, 1245 (1969)
48. J. Bijnens, J. Prades, Nucl. Phys. B **490**, 239 (1997)
49. J. Bijnens, Phys. Lett. B **306**, 343 (1993)
50. R. Baur, R. Urech, Nucl. Phys. B **499**, 319 (1997)
51. J. Gasser, H. Leutwyler, Nucl. Phys. B **250**, 517 (1985)
52. G. Passarino, M.J. Veltman, Nucl. Phys. B **160**, 151 (1979)